



CHORUS

This is the accepted manuscript made available via CHORUS. The article has been published as:

The $^{30}\text{Mg}(t,p)^{32}\text{Mg}$ “puzzle” reexamined

A. O. Macchiavelli, H. L. Crawford, C. M. Campbell, R. M. Clark, M. Cromaz, P. Fallon, M. D. Jones, I. Y. Lee, M. Salathe, B. A. Brown, and A. Poves

Phys. Rev. C **94**, 051303 — Published 18 November 2016

DOI: [10.1103/PhysRevC.94.051303](https://doi.org/10.1103/PhysRevC.94.051303)

The $^{30}\text{Mg}(t, p)^{32}\text{Mg}$ “Puzzle” Reexamined

A. O. Macchiavelli, H. L. Crawford, C. M. Campbell, R. M. Clark,
M. Cromaz, P. Fallon, M. D. Jones, I. Y. Lee and M. Salathe

Nuclear Science Division, Lawrence Berkeley National Laboratory, Berkeley, CA 94720, USA

B. A. Brown

*Department of Physics and Astronomy and National Superconducting Cyclotron Laboratory,
Michigan State University, East Lansing, MI USA*

A. Poves

*Departamento de Fisica Teorica and IFT-UAM/CSIC,
Universidad Autonoma de Madrid, E-28049 Madrid, Spain*

We propose a phenomenological three-level mixing model of unperturbed $0p0h$, $2p2h$ and $4p4h$ states, to describe the low-lying 0^+ states in ^{32}Mg . Within this approach, self-consistent solutions exist that provides good agreement with the available experimental information obtained from the $^{30}\text{Mg}(t,p)^{32}\text{Mg}$ reaction. The inclusion of the third state, namely the $4p4h$ configuration, resolves the “puzzle” that results from a two-level model interpretation of the same data. In our analysis, the ^{32}Mg ground state emerges naturally as dominated by intruder ($2p2h$ and $4p4h$) configurations, at the 95% level.

PACS numbers: 21.10.Hw, 27.30.+t, 21.10.Jx, 25.55.Hp

I. INTRODUCTION

The $N=20$ Island of Inversion has been the subject of intense work, both experimentally and theoretically [1]. As protons are removed from $^{40}_{20}\text{Ca}$, changes in the balance between the monopole shifts of the single-particle levels and the pairing plus quadrupole correlations erode the $N=20$ shell gap, leading to deformed ($2p2h$, $4p4h$) ground states in these nuclei, expected *a-priori* to be semi-magic and spherical. The nucleus ^{32}Mg takes center stage in this region, where neutron pairs promoted from *sd* to *fp* levels across the narrowed $N=20$ gap are energetically favoured. The enhanced occupation of these deformation-driving *fp* orbitals causes the nucleus to deform [2, 3].

Wimmer *et al.* [4] studied the two-neutron transfer reaction $^{30}\text{Mg}(t, p)^{32}\text{Mg}$ at CERN/ISOLDE and discovered the first excited 0^+_2 state (at 1.058 MeV), which was attributed to be largely the $0p0h$ “spherical” state. Following on these results, Fortune [5] carried out a two-level model analysis of the reaction data and put forward the puzzling conclusion that in ^{32}Mg it is the 0^+_1 ground state which is actually dominated by the *sd*-shell components ($\approx 80\%$) and the excited 0^+_2 by the *fp*-shell $2p2h$ intruder configuration, contrary to the accepted interpretation (see also Ref. [6]).

Large scale shell-model calculations [7] however, predict the coexistence of $0p0h$, $2p2h$ and $4p4h$ states in the low-lying excitation spectra of the $N \sim 20$ Mg nuclei, calling into question the validity of a two-level approach. Inspired by these results, we have revisited the analysis of Fortune [5, 8], extending it now to a three-level mixing.

II. THE APPROACH

To investigate the validity of a three-state mixing model to describe the low-energy structure in ^{32}Mg , and in particular to explain the observations of the $^{30}\text{Mg}(t, p)^{32}\text{Mg}$ measurement [4], without the complexities of a full large-scale shell-model calculation, we assume mixing between unperturbed, pure $|n\text{p}n\text{h}\rangle$ configurations, where $n = 0, 2$, and 4 . The mixing matrix is tri-diagonal, and we make the simplifying assumption that the interaction strengths between the $|0p0h\rangle$ and $|2p2h\rangle$ configurations and the $|2p2h\rangle$ and $|4p4h\rangle$ configurations are equal ($-V$). Thus, the mixing matrix has the form:

$$\begin{pmatrix} e_0 & -V & 0 \\ -V & e_2 & -V \\ 0 & -V & e_4 \end{pmatrix} \quad (1)$$

where e_0 , e_2 and e_4 are the energies of the unperturbed $0p0h$, $2p2h$ and $4p4h$ configurations respectively. At this point it is important to comment that, while one would be tempted to think that this could be equivalent to the mixing of two states, namely an spherical one ($0p0h$ configuration) and a deformed one (a combination of $2p2h$ and $4p4h$ configurations), the 3×3 matrix above does not reduce to a 1×1 plus 2×2 block sub-matrices. However, by taking the limit of the $4p4h$ at very high-energy, we do recover a 2×2 matrix and reproduce Fortune’s results.

From the diagonalization we obtain wavefunctions of the form:

$$|0^+_j\rangle = \alpha_j|0p0h\rangle + \beta_j|2p2h\rangle + \gamma_j|4p4h\rangle, \quad (2)$$

where α_j , β_j , and γ_j are constrained by the normalization condition (i.e. $\alpha_j^2 + \beta_j^2 + \gamma_j^2 = 1$).

TABLE I: Results for the wavefunction amplitudes and energies of the first three 0^+ states obtained from diagonalization of Eq. 1 for $V = 0.58$ MeV.

State	Excitation Energy [MeV]	α	β	γ
		$ 0p0h\rangle$	$ 2p2h\rangle$	$ 4p4h\rangle$
0_1^+	0.0	0.20	0.68	0.70
0_2^+	1.06	0.39	0.60	-0.70
0_3^+	2.22	0.90	-0.41	0.14

As a starting point we take the unperturbed values, based on the large-scale shell model calculations of Ref. [7], to be $e_0 = 1.4$ MeV, $e_2 = 0.2$ MeV and $e_4 = 0$ MeV.

III. CALCULATIONS AND RESULTS

Diagonalizing the matrix of Eq. 1, we directly obtain the mixed state eigenvalues as a function of the mixing matrix element V – these results are plotted in Fig. 1(a), for the ground state 0_1^+ (red), first excited 0_2^+ (green) and second excited 0_3^+ (blue). The corresponding wavefunction coefficients for these states are plotted, with the same color coding in Fig. 1(b), where α coefficients for the $|0p0h\rangle$ contribution are the solid lines, β coefficients, for the $|2p2h\rangle$ component, are dotted lines, and the γ $|4p4h\rangle$ coefficients are dashed lines.

Considering the energies of the mixed 0^+ states, we can constrain the mixing strength V according to the experimentally observed separation between the 0_1^+ and 0_2^+ states of 1.06 MeV [4]. This energy separation occurs for a mixing strength of $V = 0.58$ MeV. For this mixing strength, the corresponding energies and wavefunction amplitudes for the three 0^+ states are summarized in Table III. In particular for the ground state we have $\alpha_1 = 0.20$, $\beta_1 = 0.68$ and $\gamma_1 = 0.70$. This corresponds well to the amplitudes obtained for the ground state of ^{32}Mg using a full large-scale shell-model calculation with the SDPF-U-MIX effective interaction, where $\alpha = 0.32$, $\beta = 0.72$ and $\gamma = 0.61$ [9]. These shell-model based amplitudes are plotted as the black circles in Fig. 1.

Additional support to our approach can be assessed by looking at the overlaps of the three lowest 0^+ states obtained within the full shell model space with the lowest energy states of the three pure nph configurations. These are shown in Table II. As seen, over 90 % of the full wavefunctions come indeed from the pure configurations, and justifies the truncation to a three level model.[‡]

To make further ties with experiment and check the consistency of this simple model, we adopt a description

[‡] The initial energies of the 3x3 model that approximately reproduce these percentages for $V = 0.6$ are $e_0 = 0.69$ MeV, $e_2 = 0.0$ MeV and $e_4 = 0.15$ MeV, corresponding to unperturbed values derived from the overlaps in Table II.

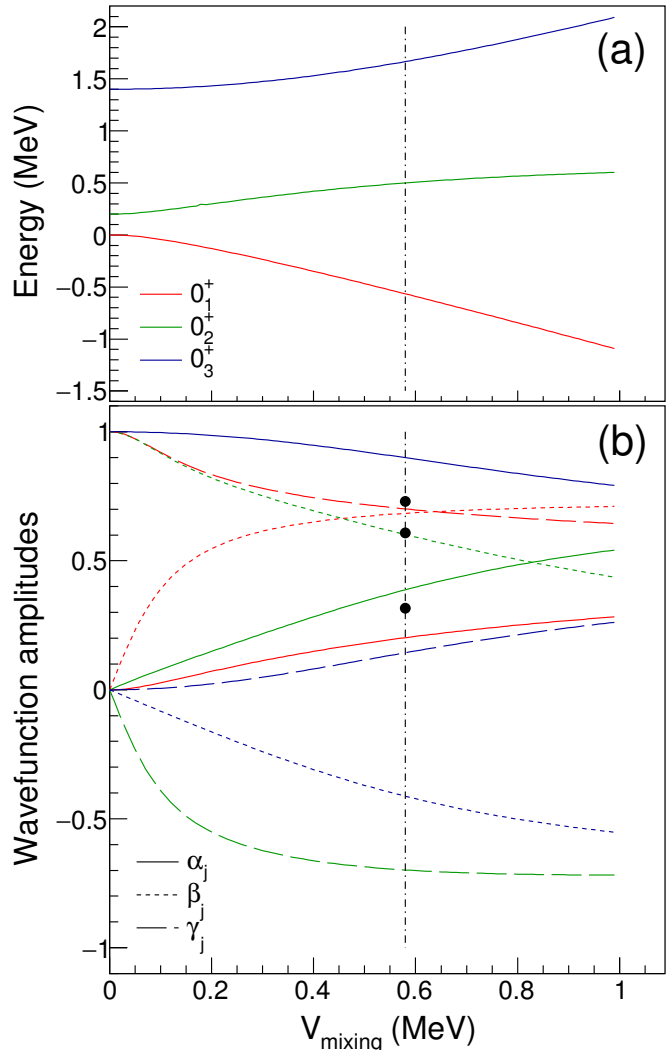


FIG. 1: (color online) Graphical illustration of the solutions for diagonalization of the matrix of Eq. 1 as a function of V . The top panel (a) shows the evolution of the energy levels for the mixed 0^+ states as a function of V . The dot-dashed line at $V=0.58$ MeV represents the interaction strength at which the excitation energy for 0_2^+ equals the experimental value. The bottom panel (b) shows the evolution of the wavefunction amplitudes for the three 0^+ states.

for the ^{30}Mg ground state as:

$$|0_1^+(^{30}\text{Mg})\rangle = \epsilon|0p0h\rangle + \sqrt{1 - \epsilon^2}|2p2h\rangle, \quad (3)$$

under the assumption that a significant $4p4h$ contribution in the ground state of ^{30}Mg is very unlikely, as this is expected to lie at much higher energy. With this description, we can calculate the cross-sections for two-neutron transfer to the ground state and excited 0^+ states in ^{32}Mg from the ground state of ^{30}Mg . The cross-section to the i^{th} 0^+ state in ^{32}Mg from the ^{30}Mg ground state can be

TABLE II: The overlaps (in percent) of the three lowest 0^+ states in the full shell model space with the lowest energy states of the three pure $npmh$ configurations.

Full/Pure	0p0h	2p2h	4p4h	Sum
1	10	53	31	94
2	32	8	53	93
3	48	31	12	91

expressed as:

$$\sigma_{0_i^+} \propto (\epsilon\alpha_i T_{0,0} + \epsilon\beta_i T_{0,2} + \sqrt{1 - \epsilon^2\beta_i T_{2,2}} + \sqrt{1 - \epsilon^2\gamma_i T_{2,4}})^2 \quad (4)$$

where $T_{a,b}$ is the two-nucleon transfer amplitude between the $|apah\rangle$ state in ^{30}Mg and the $|bpbh\rangle$ component of the wavefunction in ^{32}Mg . Referring to the schematic diagram shown in Figure 2, we note that the two-neutron transfer does not connect the ^{30}Mg $|0p0h\rangle$ wavefunction component with the ^{32}Mg $|4p4h\rangle$, nor the ^{30}Mg $|2p2h\rangle$ contribution with the ^{32}Mg $|0p0h\rangle$ wavefunction, i.e. $T_{0,4}$ and $T_{2,0} = 0$. We can further realize that the amplitudes $T_{0,0}$ and $T_{2,2}$ both correspond to the addition of a pair of sd neutrons (T_{sd}), while $T_{0,2}$ and $T_{2,4}$ relate to the addition of a pair of fp neutrons (T_{fp}), and make the simplifying assumption that $T_{0,0} = T_{2,2}$ $T_{0,2} = T_{2,4}$. This is supported if one considers the transfer amplitudes in a single particle description, which can be estimated with simple coefficients of fractional parentage and the overlap of two neutrons in the triton with the orbitals of the target nucleus [10]. In line with the arguments of Fortune [5] we further assume that $T_{fp} = R \times T_{sd}$, and used his value of $R = 2$, also validated in our approach by the experimental constraint on the total cross-section populating the 0_1^+ , 0_2^+ , and 0_3^+ states, which is 17.0(9) mb [4]. We also note that a variation of R within a factor of two (up or down) does not alter the results of the calculations described below.

A cross-section ratio equation can then be defined, which simplifies to:

$$\frac{\sigma_{0_i^+}}{\sigma_{0_j^+}} = \left(\frac{\epsilon(\alpha_i + \beta_i R) + \sqrt{1 - \epsilon^2}(\beta_i + \gamma_i R)}{\epsilon(\alpha_j + \beta_j R) + \sqrt{1 - \epsilon^2}(\beta_j + \gamma_j R)} \right)^2 \quad (5)$$

We evaluate the cross-section ratio $\sigma_{0_2^+}/\sigma_{0_1^+}$ directly as a function of V and ϵ , and obtain the results plotted in Fig. 3. Experimentally, this cross-section ratio has a value $\sigma_{0_2^+}/\sigma_{0_1^+} = 0.62(6)$ [4]. Taking our earlier result constrained by the experimental excitation energy of $E(0_2^+) = 1.06$ MeV for $V = 0.58$ MeV (Fig. 1(a), dot-dashed line), the experimental ratio is reproduced for a ^{30}Mg ground-state wavefunction:

$$|0_1^+(^{30}\text{Mg})\rangle = 0.99|0p0h\rangle + 0.17|2p2h\rangle. \quad (6)$$

The deduced amplitudes are in good agreement with those deduced from the $E0$ transition strength in ^{30}Mg [11], where $\epsilon = 0.983(15)$.

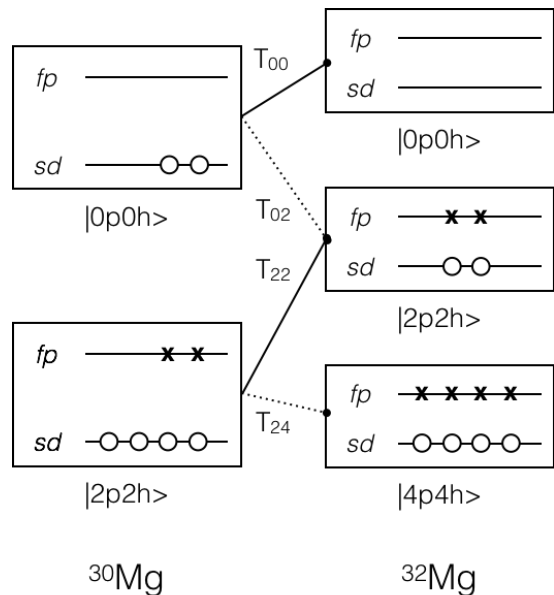


FIG. 2: Schematic representation of the two-neutron transfers under consideration. The components of the ^{30}Mg ground state wavefunction connect to components of the ^{32}Mg 0^+ wavefunctions as shown. The solid connecting lines correspond to transfer of sd shell neutrons, while the dotted connecting lines correspond to transfer of a pair of fp shell neutrons. Open circles represent holes in the sd shell, while the crosses represent particles in the fp shell.

At this point it is relevant to comment on the possible effect of the Q -value dependence of the transfer amplitudes. We have considered this effect by looking at the results of a DWBA calculation using the code DWUCK4 [12]. As could be expected, the transfer to the excited 0_2^+ state is suppressed more than the ground state, but the conclusions above do not change much. The effect can be cast in the form of a correction to the experimental cross-section ratio, making it larger. As seen in Fig. 3, this will correspond to a solution with ^{30}Mg closer to a spherical shape.

Within our model we find the ratio $\sigma_{0_3^+}/\sigma_{0_1^+}$ to be very small and consistent with the non-observation of a third 0^+ state in the work of Wimmer *et al.* [4]. To obtain a summed cross-section of $(\sigma_{0_1^+} + \sigma_{0_2^+} + \sigma_{0_3^+}) = 17.0(9)$ mb, the required normalization is $\sigma_{sd} = 3.1$ mb, in line with the expectations for pure sd neutron-pair transfer [5].

Finally, while the wavefunction above for the ^{30}Mg ground-state agrees well with the results of Ref. [11] there is some model dependence in that analysis arising from the $E0$ matrix elements used. It is possible that an equally realistic description for the structure of ^{30}Mg may be consistent with a lower $0p0h$ amplitude, down to $\approx 80\%$. We explore the existence of other solutions within our model framework, in terms of the energies of the unperturbed initial states: e_0 , e_2 , and e_4 . As seen in Fig. 4 modest changes in the initial energies allow for physically sound solutions, which reproduce the experi-

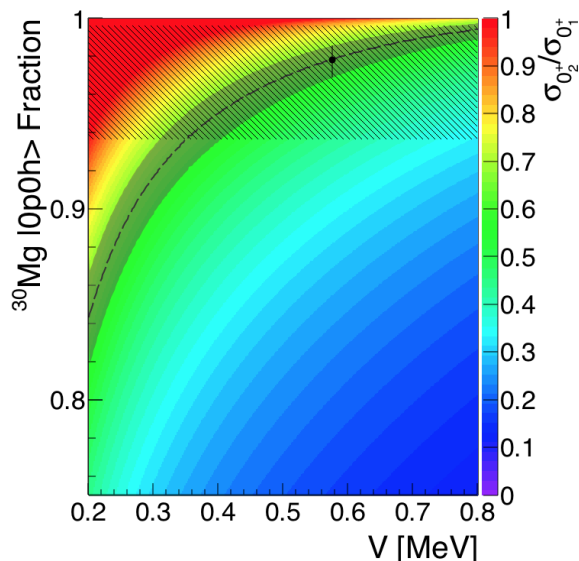


FIG. 3: (color online) Cross-section ratio $\sigma_{0_2^+}/\sigma_{0_1^+}$ calculated according to Eq. 5 based on the ^{32}Mg wavefunction amplitudes as plotted in Fig. 1(b) as a function of V and the $|0p0h\rangle$ squared amplitude in the ^{30}Mg ground state (ϵ^2 in Eq. 3). The hashed area represents the results of Ref. [11], while the dashed line and shaded error band indicate the experimental range of the cross-section ratio. The black data point indicates the mixing strength, V , which reproduces the experimental $E(0_2^+)$.

mental cross-section ratio and $E(0_2^+)$ in ^{32}Mg , and are more consistent with a ^{30}Mg ground state less strictly dominated by a $0p0h$ configuration (i.e. the region between the dashed-lines in the figure). These changes, in particular the energy of the $4p4h$ configuration, could be explained by small adjustments of the single-particle monopole shifts and the quadrupole interaction.

It is also of interest to compare the wave functions for the lowest $0_{1,2}^+$ states in ^{32}Mg obtained for solution A, with those obtained for solutions B and C, listed in Table III. Solutions B and C appear quite different from A in the figure, i.e. in the ^{30}Mg ground state wave function obtained, but the amplitudes of the ^{32}Mg wave functions are in fact quite consistent and robustly confirm its ground state as dominated by ($2p2h$ and $4p4h$) excitations.

IV. CONCLUSION

It is clear that the inclusion of the third state, namely the $4p4h$ configuration resolves the “puzzle” of ^{32}Mg proposed by Fortune [5, 8], and the ^{32}Mg ground state emerges naturally as dominated at the 95% level by intruder ($2p2h$ or $4p4h$) configurations. Within a simple three-level model, self-consistent solutions exist that provide good agreement with the experimental excitation energy of the 0_2^+ state, the cross-section ratio $\sigma_{0_2^+}/\sigma_{0_1^+}$,

TABLE III: Results for the mixing strength required to reproduce the experimental $E(0_2^+)$ and the resulting wavefunction amplitudes in ^{32}Mg corresponding to the solutions indicated by points A, B, and C in Fig. 4 with (e_0, e_2, e_4) [MeV] = (1.4, 0.2, 0.0), (1.5, 0.5, 0.0) and (1.75, 0.75, 0.0) respectively.

State	Point	V [MeV]	α 0p0h	β 2p2h	γ 4p4h
0_1^+	A	0.576	0.20	0.68	0.70
0_2^+			0.39	0.60	-0.70
0_3^+			0.90	-0.41	0.14
0_1^+	B	0.566	0.17	0.59	0.79
0_2^+			0.44	0.67	-0.60
0_3^+			0.88	-0.45	0.14
0_1^+	C	0.482	0.11	0.47	0.88
0_2^+			0.40	0.79	-0.48
0_3^+			0.91	-0.40	0.10

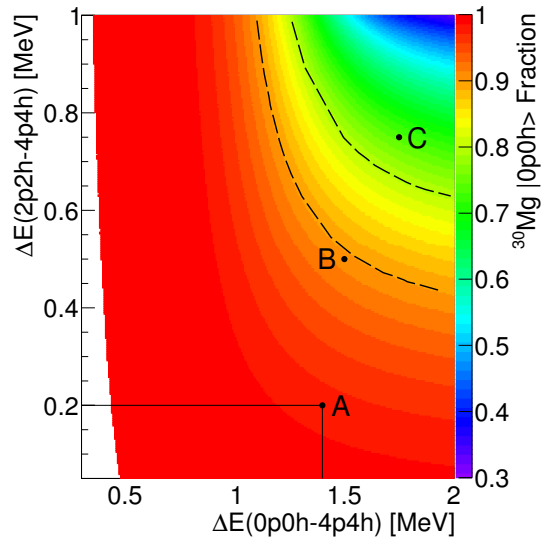


FIG. 4: (color online) Percent squared amplitude of the $0p0h$ component in the ^{30}Mg ground-state (ϵ^2 in Eq. 3) required to explain the experimental data as a function of the energies of the unperturbed states. Point A shows the solution (Eq. (6)) with the energies fixed at the unperturbed values discussed in Section II. The dashed lines indicate possible solutions with a $0p0h$ amplitude for the ^{30}Mg ground state at 80% and 90%. As discussed in the text, Points B and C are used as a reference with respect to the ^{32}Mg wave functions.

and the summed cross-section ($\sigma_{0_1^+} + \sigma_{0_2^+} + \sigma_{0_3^+}$) with a reasonable value for the cross-section for transfer of two sd neutrons. These scenarios also indicate a ^{30}Mg ground-state dominated by the $0p0h$ component, in line with experimental evidence and shell model expectations. While further experimental information, such as the lifetime of the 0_2^+ state will further constrain shell-model and more complex and complete descriptions of nuclear structure in this region, the ^{32}Mg “puzzle” is, to first order, resolved.

Acknowledgments

This material is based upon work supported by the U.S. Department of Energy, Office of Science, Office of Nuclear Physics under Contracts No. DE-AC02-

05CH11231 (LBNL), by the U.S. NSF Grant No. PHY-1404442, and by the Spanish Ministry of Ciencia e Innovación under Grant FPA2014-57196 and Programme “Centros de Excelencia Severo Ochoa” SEV-2012-0249.

-
- [1] O. Sorlin and M. Porquet, *Prog. Part. Nucl. Phys.* **61**, 602 (2008).
 - [2] A. Poves and J. Retamosa, *Phys. Lett.* **B184**, 311 (1987).
 - [3] E. K. Warburton, J. A. Becker and B. A. Brown, *Phys. Rev. C* **41**, 1147 (1990).
 - [4] K. Wimmer *et al.*, *Phys. Rev. Lett.* **105**, 252501 (2010).
 - [5] H. T. Fortune, *Phys. Rev. C* **84**, 024327 (2011).
 - [6] J. A. Lay, L. Fortunato, and A. Vitturi, *Phys. Rev. C* **89**, 034618 (2014).
 - [7] E. Caurier, F. Nowacki and A. Poves, *Phys. Rev. C* **90**, 014302 (2014).
 - [8] H. T. Fortune, *Phys. Rev. C* **85**, 014315 (2012).
 - [9] H. L. Crawford *et al.*, *Phys. Rev. C* **93**, 031303(R) (2016).
 - [10] Norman K. Glendenning, *Direct Nuclear Reactions*, Chapter 15, World Scientific Publishing Co. Pte. Ltd., Singapore, 2004.
 - [11] W. Schwerdtfeger *et al.*, *Phys. Rev. Lett.* **103**, 012501 (2009).
 - [12] P.D.Kunz, DWUCK4 Program Manual. University of Colorado. spot.colorado.edu/~kunz/DWBA.html